

# FDTD Analysis of Dielectric-Embedded Electronically Switched Multiple-Beam (DE-ESMB) Antenna Array

Junwei Lu, *Member, IEEE*, David Thiel, *Senior Member, IEEE*, and Seppo Saario, *Student Member, IEEE*

**Abstract**—The design procedure, finite-difference time-domain (FDTD) modeling, and experimental measurements for a novel dielectric-embedded electronically switched multiple-beam (DE-ESMB) antenna array are presented in this paper. Size reduction of a parasitic switched monopole antenna was accomplished by embedding the array in a cylindrical rod of L6G nylon with a relative permittivity  $\epsilon_r = 4.4$ . Dielectric-embedded and free-space prototypes of a nine-element ESMB antenna array were modeled and experimentally characterized. Experimental measurements and numerical results are in good agreement. The measured return loss for the nine-element embedded antenna was less than  $-25$  dB at 2.32 GHz. An overall volume reduction of 80% and footprint reduction of 50% was achieved. Adaptive simulated annealing with FDTD was used to optimize the 17-element DE-ESMB array, achieving a return loss of less than  $-10$  dB across the 2.4 GHz to 2.5 GHz ISM band.

**Index Terms**—Dielectric embedded antenna array, electronically switched multiple beam, FDTD analysis, smart antenna.

## I. INTRODUCTION

IN MOBILE terminals, the size of the antenna is important, as portability is a key requirement. The rapid growth of the wireless market has resulted in new technologies being investigated to improve performance and usage of the available spectrum in the most efficient way. Smart antennas with controllable directionality are one promising candidate as they allow higher reuse of channels and increased system performance. Phased array antennas can also be considered. However, they typically require an interelement spacing of greater than  $0.5\lambda_0$ . In switched parasitic arrays, the separation distances can be reduced to  $0.3\lambda_0$  [1]. The structure lies on a finite ground plane as shown in Fig. 1(a).

The characteristics of a nine-element dielectric-embedded electronically switched multiple-beam (DE-ESMB) antenna array are initially investigated. This antenna can produce two beams simultaneously, separated by  $180^\circ$ , with four possible beam directions at  $90^\circ$  spacing through the azimuthal plane. The center element is slightly longer than a resonant quarter wavelength element and is shorted to the ground plane giving the array Yagi-Uda characteristics. The center element is surrounded by elements placed along two radially concentric circles. These elements can be switched to a number of possible

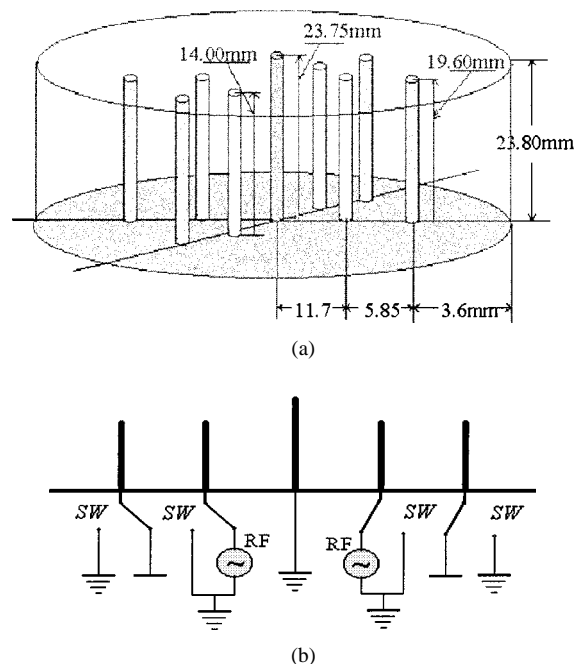


Fig. 1. Geometry of the dielectric embedded antenna array. (a) Configuration of DE-ESMB antenna array. (b) Switching circuits for beam control.

different states. The inner circle of elements may be either active elements, passive elements shorted to ground, or passive elements isolated from the ground plane. The outer circle of elements are always parasitic, but can be switched from open circuit to short circuit. Each circle has the same number of elements. The switching can be achieved electronically using active semiconductor devices (p-i-n diode or field-effect transistor switches) or by radio frequency microelectromechanical systems (RF MEMS) switches as shown in Fig. 1(b).

This work extends our earlier work on small switchable antenna arrays for mobile communications [1]–[2]. The size reduction was achieved by embedding the switched parasitic array in a homogeneous dielectric material. Small antenna design processes and analysis concepts are developed to analyze the problem based on computer modeling and optimization techniques. Generally, the design of new radio frequency/microwave (RF/MW) electromagnetic devices requires several design iterations to achieve an acceptable solution, as do computer-aided design/computer-aided engineering (CAD/CAE) based design techniques. Sometimes conventional CAD/CAE based design processes can be much slower than experimental work if the CAD/CAE does not incorporate any effective

Manuscript received July 5, 2001.

The authors are with the School of Microelectronic Engineering, MCE, Griffith University, Brisbane QLD 4111, Australia (e-mail: J.Lu@mc.gu.edu.au; D.Thiel@mc.gu.edu.au; saario@ieee.org).

Publisher Item Identifier S 0018-9464(02)01146-9.

optimization techniques. This paper will discuss the size reduction of a DE-ESMB antenna using an optimizing design process. It also provides a general design process for RF/MW electromagnetic device design in terms of CAD/CAE and optimization approaches.

## II. BASIC DE-ESMB ANTENNA-SIZE REDUCTION CONCEPTS

It is well known that by embedding a wire in a dielectric medium, the electrical length of a wire antenna can be reduced [3]. If the dielectric is of infinite extent, then the wavelength of radiation in the medium is given by  $\lambda_r = \lambda_0 / \sqrt{\epsilon_r \mu_r}$ , where  $\epsilon_r$  is the relative permittivity and  $\mu_r$  is the relative permeability of the material. If the antenna elements are embedded in a high permittivity medium (nonmagnetic material) of infinite extent, the wavelength in the medium can be rewritten as  $\lambda_r = \lambda_0 / \sqrt{\epsilon_r}$  and the size reduction factor  $F_r$  for the length of antenna elements will be

$$F_r = \sqrt{\epsilon_r}. \quad (1)$$

To reduce the total volume and weight of the DE-ESMB array, the radius of the dielectric from outer element to air interface should be smaller than the height of dielectric. In a practical antenna, the reduction factor will not be as great as  $F_r$  as the embedding dielectric will not be of infinite extent. Clearly, the reduction function will be a function of the shape, size, electrical characteristics of the dielectric material, and the location of each wire element in the material. Thus, the actual reduction factor  $F_{ra}$  for the size of antenna will be

$$F_{ra} = f(\sqrt{\epsilon_r}, h, r_1, r_2, r_3, l_1, l_2) \quad (2)$$

where  $h$  is the height of dielectric,  $r_1$  is the radius of inner element circle,  $r_2$  is the radius of outer element circle,  $r_3$  is the radius of embedding dielectric,  $l_1$  the length of the elements on the inner circle, and  $l_2$  the length of the elements on the outer circle respectively.

## III. COMPUTATION MODEL OF DE-ESMB ANTENNA ARRAY

Unlike the free-space ESMB antenna arrays, the switched parasitic and active elements of the DE-ESMB array are embedded in a cylinder of high permittivity dielectric material, the physical size has to be optimized due to complex wave interaction of radiation between elements, and the dielectric/air interface of the cylinder.

Since there are no design rules for such DE-ESMB antenna arrays, the only way to achieve an optimal antenna is to use a full wave numerical solution and control it with a robust optimization algorithm. In this paper, we used the finite-difference time-domain (FDTD) method, as it is well suited to modeling complex objects, being able to include finite dielectric media, thin wires, and lumped loads. Parameters of interest that can be derived from FDTD simulations include broad-band input impedance, radiation patterns, and time harmonic current densities. Finite-element method and FE-TD based numerical methods are also applicable to this type of problem. However, FDTD uses comparatively less computer memory during the

computation and, having access to source code, it is easily integrated into an optimizing design procedure. The FDTD method is based on Maxwell's curl equations as shown in (3)

$$\begin{aligned} \frac{\partial \vec{H}}{\partial t} &= -\frac{1}{\mu} \nabla \times \vec{E} - \frac{\rho'}{\mu} \vec{H} \\ \frac{\partial \vec{E}}{\partial t} &= \frac{1}{\epsilon} \nabla \times \vec{H} - \frac{\sigma}{\epsilon} \vec{E}. \end{aligned} \quad (3)$$

The system of six coupled partial differential equations in the Cartesian coordinate system forms the basis of the FDTD numerical algorithm for electromagnetic wave interactions with general three-dimensional (3-D) objects [4]. The size of the simulation domain was  $120 \times 120 \times 60$  cells with a space discretization of 1 mm per cell. The time step was set to the Courant stability limit.

Berenger's original split-field perfect matching layer (PML) absorbing boundary conditions (ABC) were implemented with separate memory allocation domains between the FDTD and PML regions to reduce memory requirements [4] since standard FDTD only requires six field components per cell whereas PML require 12 fields per cell. The PML ABC was four cells deep with a parabolic conductivity profile with  $R(0) = 1e-5$ .

A subcellular thin-wire model was used to include the effects of thin wires in the simulation [x], the wire diameter was specified to be 0.9 mm. To obtain broad-band impedance results, a Gaussian pulse  $p(\tau)$  was used to excite the base of a resistively loaded monopole element [x]

$$p(\tau) = \begin{cases} e^{-\alpha(\tau-\tau_0)^2}, & 0 \leq \tau \leq 2\tau_0 \\ 0, & \text{otherwise.} \end{cases} \quad (4)$$

The impedance was calculated using  $Z(\omega) = V(\omega)/I(\omega)$ , where the voltages and currents are recorded at the base of the feed monopole and transformed into the frequency domain using a fast Fourier transform. In this simulation, only one port is connected to the source and the others are either open circuit or short-circuited, only one port, on the opposite the reflector with respect to the feed is terminated in a  $50\text{-}\Omega$  load. A frequency domain far-field transform was used using the surface equivalence principle whereby currents on a virtual box within the FDTD simulation domain are transformed to the far field via the free-space Green's function [4]. Time harmonic magnetic field strengths were calculated using a running discrete Fourier transform at a frequency of 2.45 GHz. Time-stepping was completed after 3000 time steps, ensuring that all fields in the simulation region had decayed to zero. Typical execution times for the simulations were in the order of 39 min on an AMD Thunderbird at 1380 MHz, including post processing, and the core FDTD update routine had a cell calculation rate of  $1.433 \times 10^6$  cells per second.

## IV. EVALUATION OF SIZE-REDUCTION FACTORS AND CONSTRAINTS FOR OPTIMAL DESIGN PROCESS

The optimal design is often involved in defining or determining the objective functions and constraints. The resonant

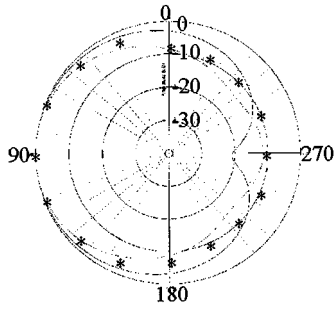


Fig. 2.  $H$  plane radiation pattern at 2.4 GHz, where — — — line indicates the free space antenna and — line indicates the dielectric embedded antenna. \*\*\*\* line indicates the simulation result of DE-ESMB antenna.

frequencies of the antennas and the required electrical characteristics are not achievable at the minimum volume of the antenna structure. The objective functions and physical limits (constraints) should be defined before applying the optimized design process to DE-ESMB antenna array design.

It was found that several factors significantly affect the design. These include the height of elements and diameter of dielectric block, the volume of antenna, the separation and height of the elements, and the dielectric constant. In fact, the element spacing between the center reflector and inner circle elements and between the inner circle elements and outer circle elements could be initially designed to follow the dielectric scaling factor assuming a dielectric material of infinite extent. However, this is an oversimplification and the spacing between the outer elements and air interface must be optimized. Compared to the free-space ESMB antenna array, about 50% size reduction and 80% volume reduction was achieved using a L6G Nylon rod of permittivity  $\epsilon_r = 4.4$  and the assumption of the material being lossless for the simulations. The diameter and height of dielectric for the nine element antenna array is 43.3 and 23.80 mm, respectively (ESMB antenna array in air has a diameter and height of 96 and 40 mm, respectively). A manually optimized dielectric embedded antenna array, which indicates the design must be optimized for the return loss, resonant frequency, input impedance, and radiation pattern as well. All elements in the array had a diameter of 0.9 mm. The separation between center and inner elements is 11.7 mm, between inner and outer elements is 5.85 mm, and between outer and dielectric to air interface is 3.6 mm. Thus, the DE-ESMB antenna array as shown in Fig. 1 has a significant size and volume reduction.

The  $H$  plane radiation pattern obtained from FDTD simulation at 2.4 GHz is shown in Fig. 2. This demonstrates that the dielectric embedded ESMB antenna array has significant directionality. The front-to-back (FB) ratio at 2.4 GHz is  $-22$  dB for dielectric embedded ESMB antenna arrays. The  $-3$ -dB beamwidth for the dielectric embedded ESMB antenna array is  $80^\circ$ . Fig. 3 shows the FDTD simulation result compared with experiment results where the double-side print circuit board substrate and connectors are used, which shifted the resonant frequency from 2.4 to 2.32 GHz [5].

From the above investigations, we found that the height of dielectric basically is dominated by the central grounding element that basically follows the reduction factor (4). Thus, we can simplify the optimized simulation problem by fixing the height of

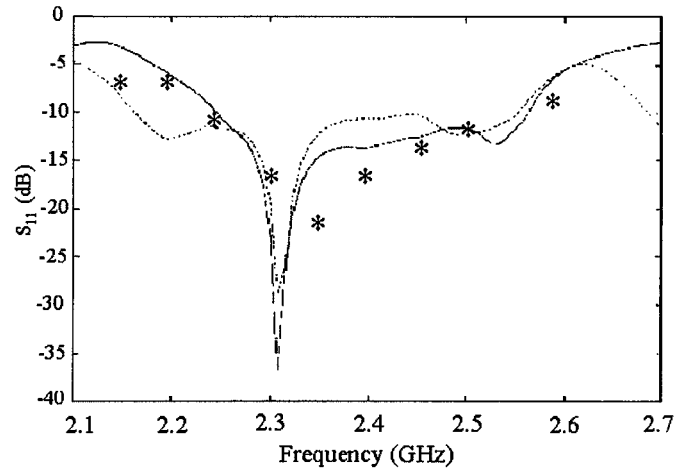


Fig. 3. Return losses for nine-element DE-ESMB antenna, where — — — line indicates the experiment result of free space ESMB antenna, — line indicates experiment result of DE-ESMB antenna, \*\*\*\* line indicates the simulation result of DE-ESMB antenna.

dielectric and dielectric constant. If we consider the return loss  $S_{11}$ , the FB ratio for the radiation pattern  $R_{fb}$ , antenna gain  $G_0$ , beamwidth of directional radiation pattern  $f_{bw}$ , and the volume of the DE-ESMB antenna as the objectives Vol, then we will have the following multiple objectives:

$$P = P_0(S_{11}, R_{fb}, G_0, f_{bw}, \text{Vol}) \quad (5)$$

where all constraints are constants and will be set up for required values. The objective function used for these optimizations was a subset of the above, only optimizing for return loss and FB ratio as follows:

$$P = P_0(S_{11}, R_{fb}, \text{Vol}).$$

Based on above investigation, we found that this is a typical constrained optimization problem. Therefore, the basic design process for DE-ESMB antenna array can be suggested as follows.

- 1) Define the design and analysis problem (DE-ESMB antenna design and simulation).
- 2) Decide what output data are required to specify a solution to the problem (small size and satisfy various the antenna performance requirements).
- 3) Decide what input data are required to formulate the problem (antenna initial size, materials, and excitation)
- 4) Develop computational models that can be used to obtain the required output from the input data (3-D structure with excitation and PML boundary conditions).
- 5) Use the computational models to obtain a solution for a given set of input data, post processing as required.
- 6) Evaluate the solution in terms of the constraints and criteria (check the results, such as the return loss  $S_{11}$ , radiation pattern  $R_{fb}$ , antenna gain  $G_0$ , and beamwidth  $f_{bw}$  from the solution).
- 7) Repeat Steps 4, 5, and 6 as necessary to obtain a satisfactory solution

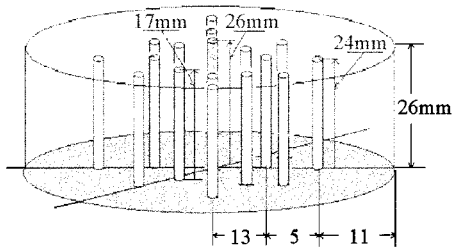


Fig. 4. Element configuration of 17-element antenna.

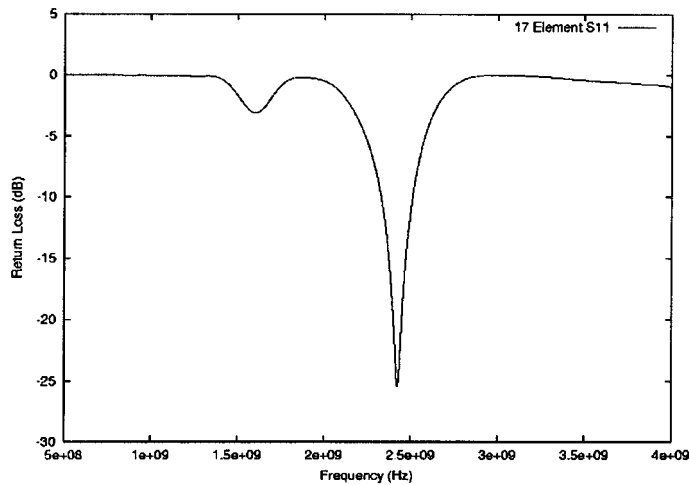


Fig. 5. Return loss of 17-element ED-ESMB antenna array.

The constrained optimization of a design requires Steps 4, 5, 6 and 7 of the design process above.

## V. SIMULATION WITH OPTIMIZATION ALGORITHM

Based on initial approach of defining the objective functions and constraints in terms of optimal design, a 17-element DE antenna array are used as a design model. The constrained optimization design process using FDTD method combined with an adaptive simulated annealing optimization algorithm is employed (see [6] for the detailed). The optimized solution model of 17-element DE-ESMB antenna array has achieved over 80% volume reduction compared with the free-space wire ESMB antenna array. The optimized physical size of the solution model is shown in Fig. 4, where a return loss of  $-25$  dB and FB ratio

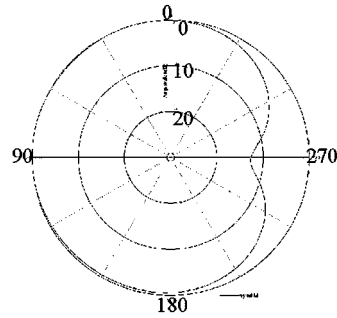


Fig. 6.  $H$  plane radiation pattern from 17-element DE-ESMB antenna array.

of 20 dB were considered to be an optimal solution as shown in Fig. 5 and 6.

## VI. CONCLUSION

The physical size of a DE-ESMB antenna array can be significantly reduced by using a dielectric embedding material. A nine-element free-space and dielectric-embedded array was modeled and experimentally measured. Good agreement was found between the numerical model and experiment. The measured return loss for the nine element DE-ESMB was less than  $-25$  dB at 2.31 GHz.

A constrained optimization design procedure was used to optimize the characteristics of a 17-element DE-ESMB antenna. The FDTD results converged to a final solution, which gives better than  $-10$  dB return loss through the 2.4–2.5-GHz band with a FB ratio of 12 dB.

The nine- and 17-element DE-ESMB antennas are significantly smaller than their free space counterparts and, as such, are more applicable for mobile terminals.

## REFERENCES

- [1] S. Preston, J. Lu, and D. Thiel, "Systematic approach to the design of directional antennas using switched parasitic and switched active elements," in *Proc. APMC*, Dec. 1998, pp. 531–534.
- [2] D. V. Thiel, S. G. O'Keefe, and J. W. Lu, "Antennas for use in portable communications devices," U.S. Patent 6 034 638, Mar. 2000.
- [3] K. Fujimoto *et al.*, *Small Antennas*. Hertfordshire, U.K.: Research Studies Press, 1987, pp. 195–261.
- [4] A. Taflov, *Computational Electromagnetics, The Finite-Difference Time-Domain Method*. Norwood, MA: Artech House, 1995.
- [5] B. Hanna, "IAP II Rep.," Griffith Univ., Brisbane, Australia, July 2000.
- [6] Adaptive simulated annealing method. [Online]. Available: [www.in-gber.com](http://www.in-gber.com)